

Laser etching technique using bubble jet impact for glass substrates

Tsu-Shien Weng · Chwan-Huei Tsai

Received: 28 June 2014 / Accepted: 27 November 2014 / Published online: 6 December 2014
© Springer-Verlag Berlin Heidelberg 2014

Abstract The purpose of this paper is to propose a new laser etching technique using bubble jet impact for glass substrates. An Nd:YAG laser is applied to the backside of the substrate which is partially submerged in water. A metal plate is placed below the glass substrate. The metal vaporizes the water and generates a turbulent bubble flow. The bubble nozzle is proposed to enhance the impact of the bubble jet. The glass surface will first be softened, and then expelled by the shock wave resulting from the jet impact. The phenomena of bubble nucleation, growth, collapse, and jet impact were studied in this paper. The formation of the etching cavity can be divided into three types: double-petal, triple-petal, and four-petal. The etching pits expanded and combined to form a complete cavity. The needed laser power does not exceed 5 W. The proposed laser etching method was successfully demonstrated for etching a cavity of 5–20 μm in depth and 50–250 μm in diameter. The bubble jet of the small nozzle diameter is well concentrated, creating a strong jet impact on the glass surface. A greater nozzle depth can enhance the impact of the bubble jet. The proposed etching technique has great potential to provide an improved solution for the micro-machining of glass.

1 Introduction

The development of microstructure machining techniques for micro-optical elements and micro-patterns has made

great progress in recent years. Photolithography is the most common technique for the manufacture of grating displays, micro-arrays, micro-lenses, micro-holes, and micro-channels. However, because it is a continuous chemical process, photolithography may result in contamination. Hence, laser etching, which does not use chemicals, offers great potential for the micro-machining of glass.

The most common type of laser used in laser etching is a UV laser. Laser etching is difficult with transparent materials because of the small absorption of the laser energy. The transmittance of the fused silica glass is $> 90\%$ over the 370 nm wavelength. Laser light absorption at wavelengths shorter than 300 nm is suitable for most applications.

Laser etching techniques are divided into dry etching and wet etching. In dry etching technique, which has been widely exploited for more than two decades, the material ablation is due to the vaporization by laser radiation. Wet etching, by contrast, uses a liquid to enhance the etching quality and reduce the thermal effect. In the dry etching process for glass, an Excimer laser has been used to etch the glass [1, 2]. The absorption of an ultraviolet laser for glass is dependent on the surface roughness. In the initial stages, the glass surface is subjected to the laser radiation, and the surface will roughen. Laser absorption then increases rapidly. The etching rate increases greatly after surface roughening.

An alternative technique of laser etching proposed by Wang et al. [3, 4] has been widely applied in glass etching. The desired etching surface of glass is placed contact with an organic solution. The hydrocarbon solution absorbs the UV laser energy. The laser-induced quick vaporization of the organic solution results in surface softening and erosion. Since the laser is applied from the backside of the transparent substrate, the technique is called laser-induced backside wet etching (LIBWE).

T.-S. Weng · C.-H. Tsai (✉)
Department of Mechatronic Engineering, Huaan University,
No. 1, Huaan Rd., Shihding District, New Taipei City 22301,
Taiwan
e-mail: chtsai@cc.hfu.edu.tw

In recent years, the LIBWE technique has been widely used in glass etching using an Excimer laser or Nd:YAG laser with frequency multiplication [5–7]. The laser heats the liquid up to the softening point of the glass. The glass materials near the interface of the glass and liquid are softened. The softened materials are then expelled by the mechanical stress resulting from the rapid heating, shock waves, and bubble flow [8, 9]. The explosive vaporization induces bubble formation and shock wave. The decomposition of the organic molecules also modifies the surface character, which can improve the absorption of laser energy at the liquid–solid interface [9].

The implementation of the LIBWE technique is complicated because of the need for a liquid absorber. An alternative technique, laser-induced backside dry etching (LIBDE), has been developed [10]. In LIBDE, a solid film substitutes for the liquid absorber. The experimental arrangement of LIBWE is more complicated than that of LIBDE. However, its etching rate with increasing pulse number is more stable than that of LIBDE [11].

LIBDE is more effective and simple than laser wet etching. The desired etching surface is coated a thin metal film, and then, the laser is applied from the backside of the glass. The thin metal film can be silver, aluminum, or copper, and its thickness is only about 100 nm [12]. The etching rate and the threshold depend on the thin film material [12]. A thin film of Cr can be used as the laser absorber [13]. The high temperature and high pressure of the Cr induce cracking on the surface of the glass substrates. These cracks grow deeply to form the surface ablation.

Etching efficiency degrades with repeated exposure of the laser. The surface of the silica substrate is modified after the first pulse, and the second pulse can etch the substrate [14]. Combining laser etching and chemical etching can improve the absorption of the glass substrate, due to chemical reactions [15, 16].

Water cannot be heated by an Nd:YAG laser or UV laser for low absorption. However, water can be vaporized at the instant of laser application to the interface of the solid and liquid. Bubbles are generated from the interface. The pressure of the bubble can reach about 1–5 MPa [17]. When a thin water film is placed on the metal plate, rapid boiling and vaporization occur at the instant of laser application [18]. Plasma and vapor bubble are generated from the submerged aluminum plate subjected to an Nd:YAG laser application. Strong shock wave emitting follows the plasma formation. The bubble shape change is a continuous cycle of expansion and collapse [19, 20].

A full understanding of water jet and bubble development can be obtained using high-speed photography [21, 22]. In recent years, the phenomena resulting from a liquid jet induced from a bubble close to a rigid boundary have been studied [23–27]. When a bubble occurs near a plate

with a small hole, the bubble will collapse and split into a liquid jet. The liquid jet enters the hole and generates a micro-pumping effect. The bubble can be generated by a laser and other means. The hole diameter of the rigid plate and the distance between the plate and the bubble are the major factors in the bubble pumping effect [27, 28].

Conventional LIBWE technique requires a laser absorber such as an organic solution to absorb the laser energy. In this study, an alternative LIBWE technique without the assistance of organic solution was proposed. The proposed technique uses an Nd:YAG laser to heat a metal plate underwater to generate the water bubbles. The idea of a bubble-induced jet pump is also applied to the laser etching of glass. A bubble nozzle is introduced to enhance the pumping effect. The material ablation mechanism of the present method is different from that of conventional LIBWE.

An ultraviolet laser is needed in the conventional laser ablation of glass. But for the proposed technique using the bubble jet to etch the glass surface, a simpler laser such as near-infrared laser can satisfy the etching requirement. This innovative approach offers great potential for laser etching of glass.

2 Principle of laser etching

2.1 Laser etching system and substrates

Figure 1 shows the configuration of the LIBWE system. For this study, the glass substrate was placed in water. The desired etching surface is in contact with the water, and the laser is applied from the backside of the glass substrate. A pulsed Nd:YAG laser was used in this study. The glass was fused silica glass, AMLCD Eagle²⁰⁰⁰, produced by the Corning Company (Taiwan). The glass thickness was

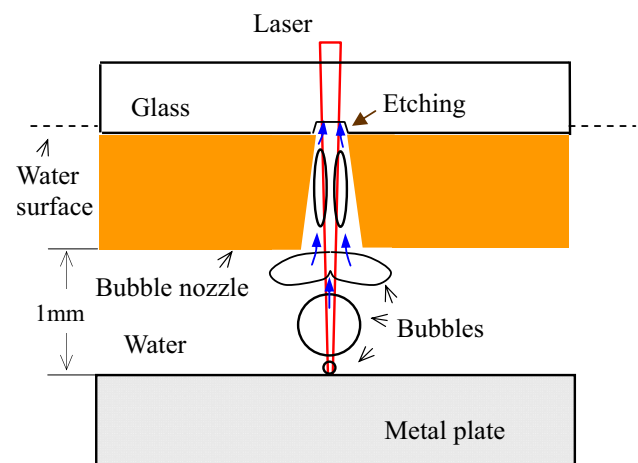


Fig. 1 Configuration of the laser-induced backside wet etching system

0.63 mm. The wavelength of the Nd:YAG laser was 1064 nm. The focal length of objective lens was 100 mm, and the minimum diameter of the focused spot was 40 μm .

A bubble nozzle was placed below the glass substrate and in direct contact with the glass surface. A metal plate made of SUS304 stainless steel was placed 1 mm below the nozzle inlet. The laser focal plane was on the surface of the metal plate. The bubbles flowed through the nozzle and induced a jet impact which ablates the glass surface.

The Nd:YAG laser power measured at the metal plate under the glass and water decreased 10 %, meaning that 90 % of the laser energy was absorbed by the metal plate. The metal vaporizes the water and generates a turbulent bubble flow. Because the laser power used is small, below 5 W, the laser ablation effect on the metal plate can be ignored.

2.2 Bubbles nucleation and growth

The bubbles generated from the surface of metal plate are the main contributor to the etching process. Figure 2

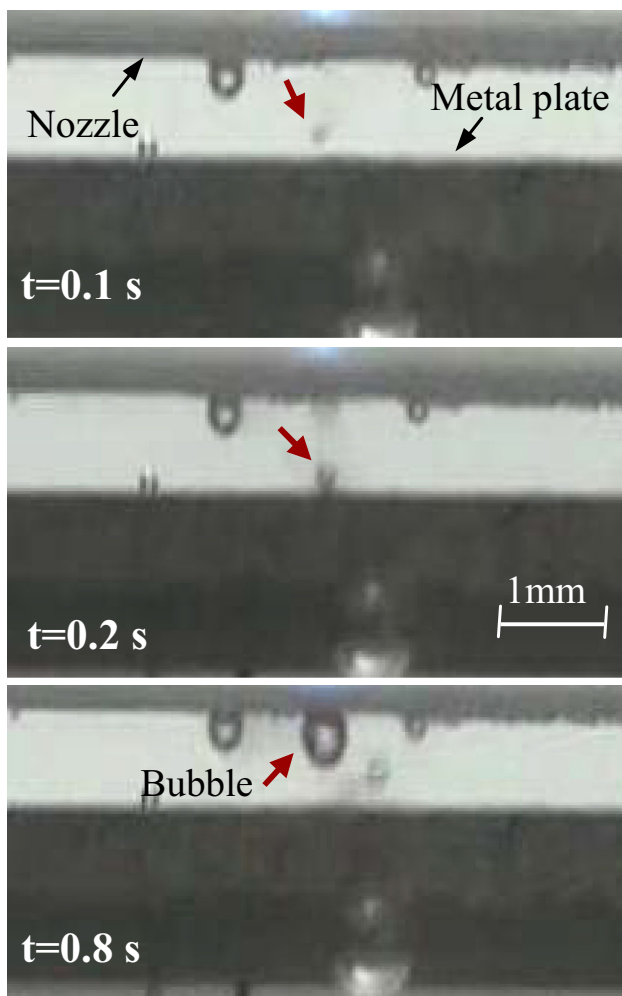


Fig. 2 Images of bubble nucleation and growth

presents the process of bubble nucleation and growth. It illustrates the interaction between the Nd:YAG laser, stainless steel, and the water. When the laser is applied to the stainless steel through the glass and water, it can induce rapid heating due to the strong absorption properties of the stainless steel.

Figure 2 shows the images of the bubble grabbed at the time of 0.1, 0.2, and 0.8 s for the laser power of 5 W at a repetition rate of 2 kHz. The bubble indicated in red arrow was initiated from the plate surface within 0.1 s. The diameter of the bubble is about 0.1 mm. The bubble size then increased rapidly. The bubble detached from the metal plate and rised up to the nozzle inlet in high speed. At the position of the nozzle inlet, the diameter of the bubble increased to 0.5 mm.

If the laser light propagates through the bubble, the refraction and reflection occur. According to the study of Lazic et al. [19, 20], the laser light refracts at the curved interface between the bubble and water. The defocusing effect is stronger for shorter wavelength. In this study, the defocused affection can be neglected for the longer wavelength, 1,064 nm, and the bubbles were confined at a very narrow region, depth of 1 mm between the metal plate and the nozzle inlet. According to the study of Lazic et al. [29], the laser reflected loss is below 2 % for the laser propagation through laser formed bubble. There was no obvious influence due to the laser–bubble interaction in this study.

2.3 Jet impact of bubble nozzle

The diffusion of the bubble flow makes the etching poor and inefficient. Therefore, the bubbles generated from the metal plate must be conducted and concentrated on the desired etching position. A bubble nozzle can enhance the strength of the bubble jet impact and confine the jetting direction. Figure 3 gives the configuration of the bubble

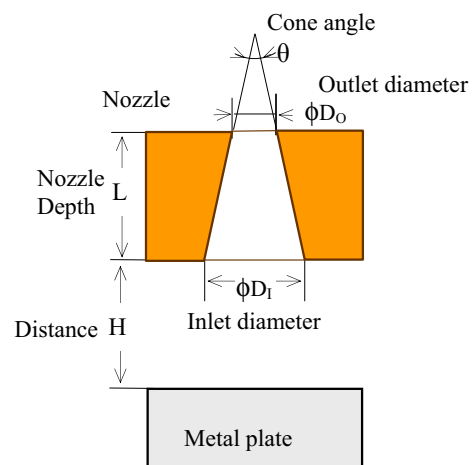


Fig. 3 Configuration of bubble nozzle and metal plate

nozzle. The parameters of nozzle geometry are the inlet diameter D_I , outlet diameter D_O , cone angle θ , and the nozzle depth L . The nozzle geometry and the distance, H , between the nozzle inlet and the metal plate dominate the impact effect of the bubble jet. For a cone angle $\theta = 0$ in which the outlet diameter equals the inlet diameter, the bubble nozzle is a cylindrical type. When the outlet diameter is less than the inlet diameter, the bubble nozzle is a conical type. The diameter of the nozzle must be larger than that of laser beam to prevent damage to the nozzle.

According to the study of micro-pumping effect by Khoo et al. [27] and Lew et al. [28], when a bubble moves close to a plate hole, the bubble will collapse and jet into the hole. The micro-pumping theory can be used to explain the principle of bubble jet impact in this study. The bubbles initiate from the metal plate surface and rise up to the nozzle inlet as shown in Fig. 2. The bubble moves close to

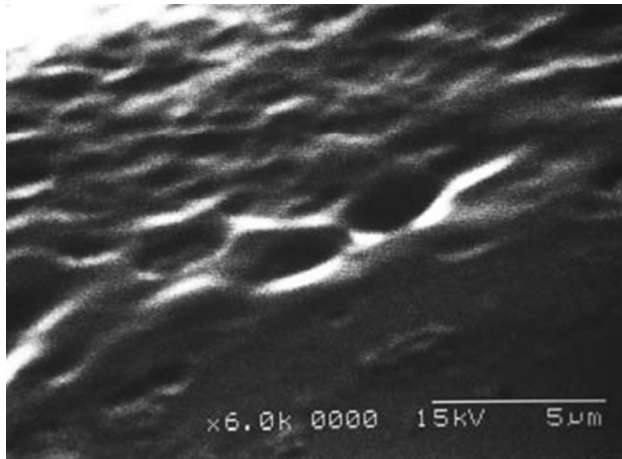


Fig. 4 SEM image of the roughened surface of the glass after bubble jet impact

the nozzle the bubble will collapse and jet into the nozzle outlet at a high speed as shown in Fig. 1. The bubble nozzle can confine the bubble jet to the desired etching region, yielding the best etching geometry. The strength of the jet impact is also enhanced by the nozzle. Without the assistance of the nozzle, the laser power required for etching may increase by a factor of ten.

Because the initial etching pit is very shallow, the laser path and beam profile have no change after laser beam propagating through the initial etching pit. If the laser path is changed, the nozzle will be damaged. But in this study, the nozzle damage has not ever been found.

2.4 Mechanism of laser etching

The mechanism of material ablation is softening and rupture by the impact of bubble jet. The glass surface will be roughened due to the impact of the bubble jet. In order to understand the mechanism of glass softening, an experiment of glass surface modification by laser was performed. An Nd:YAG laser of 5 W was applied on the glass surface, which was in contact with water. During the period of 1 min, there was no bubble generation and no roughening or etching effect on the glass surface. However, if the metal plate and nozzle are used to generate bubble jet impact on the glass surface, the roughening and etching occur.

Figure 4 shows an SEM image of the glass surface after the bubble jet impact at a laser power of 5 W. The etching surface has a smooth, soft appearance, free from any brittleness or breakage. The temperature of the bubble is not high enough to soften the glass. The laser absorption of the glass increases after glass roughening, and the roughened glass softens after absorbing the laser energy. The softened glass material may be expelled by the mechanical force of the bubble jet impact.

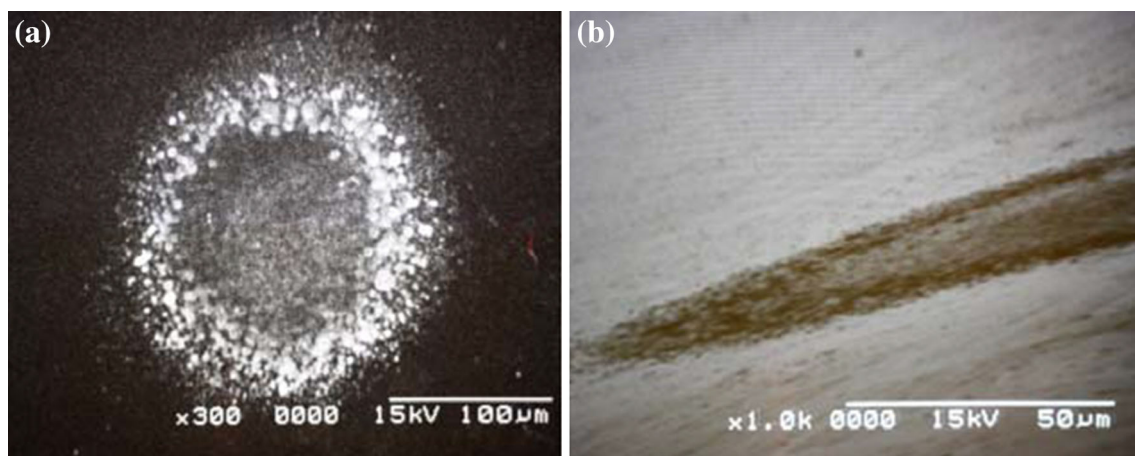


Fig. 5 SEM images of the laser etching surface with the **a** top view and **b** oblique view

3 Experiment of laser etching

3.1 Laser etching with cylindrical nozzle

A cylindrical nozzle whose nozzle outlet was in direct contact with the glass surface was used. The nozzle depth was 0.5 mm, and the diameter was 0.4 mm. The metal plate was placed 1 mm beneath the nozzle inlet. Figure 5 presents SEM images of the laser etching at a laser power of 3 W at 2 kHz. The surface ablation is circular. The diameter and the depth of the etching cavity are 120 and 6 μm , respectively. The etching depth was measured by optical microscope. Focus on the etching cavity bottom and the glass surface, and measure vertical distance between them by turning the adjustment knob of focus.

In the following laser etching experiments, the laser power was 5 W at a repetition rate of 2 kHz, and a pulse width of 150 ns. The metal plate was placed 1 mm beneath the nozzle inlet. The nozzle outlet was attached on the glass surface. The relationships between the etching diameter, nozzle depth, and laser application time for nozzle diameters of 0.25, 0.5, and 0.7 mm are shown in Fig. 6. The nozzle depths were 0.4, 0.6, 0.8, 1.0, and 2.0 mm.

In general, the etching threshold is about 1–2 s. After that time, the etching diameter begins to gradually increase. When the nozzle depth is greater, the etching diameter is larger. For a nozzle diameter of 0.25 mm, the etching diameter obtained was about 75–250 μm , while for a diameter of 0.7 mm, the etching diameter decreased to 50–150 μm . When the nozzle diameter is smaller, the etching effect is better. In general, the etching diameter for a nozzle diameter of 0.7 mm is less than that of smaller nozzle diameters of 0.25 and 0.5 mm. A smaller nozzle diameter and greater nozzle depth obtain better etching efficiency and quality.

Many experiments for different nozzle dimension were performed in this study. It was found that the bubble jet is weak for the nozzle diameter greater than 0.7 mm. For nozzle diameter < 0.25 mm, the nozzle could possibly be damaged due to the laser. The bubble jet of the small nozzle diameter is well concentrated, creating a strong jet impact on the glass surface. A greater nozzle depth can enhance the impact of the bubble jet.

3.2 Laser etching with conical nozzle

In the laser etching experiments with a conical nozzle, the laser power was 5 W at a repetition rate of 2 kHz, and a pulse width of 150 ns. The metal plate was placed 1 mm beneath the nozzle inlet. The relationships between the etching diameter, nozzle depth L , nozzle cone angle θ , and laser application time for nozzle outlet diameter of 0.4 and

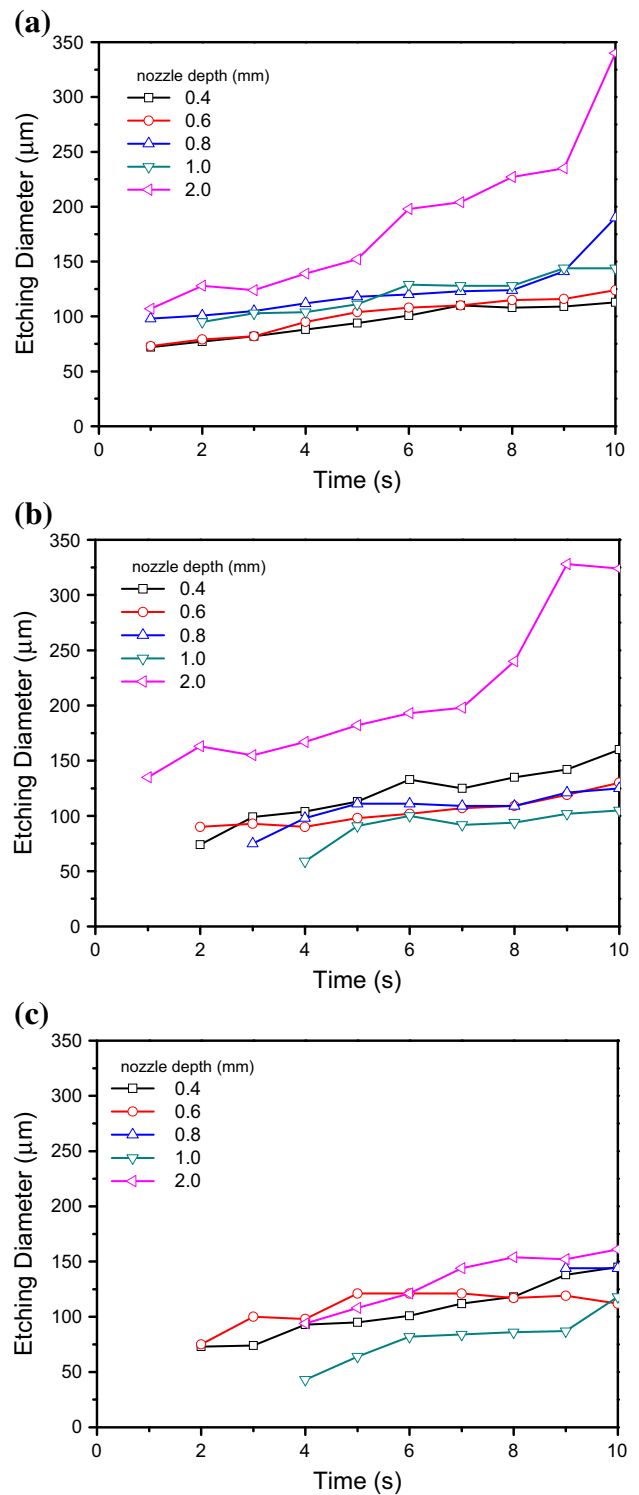


Fig. 6 Etching diameter of the glass for the cylindrical nozzle with a diameter of **a** 0.25 mm, **b** 0.5 mm, and **c** 0.7 mm

0.6 mm are shown in Fig. 7. The nozzle depths were 0.5 and 2.0 mm. The cone angles were 10° and 20° .

As shown in Fig. 7a, for an outlet diameter of 0.4 mm, and a cone angle of 10° and 20° , the etching diameter

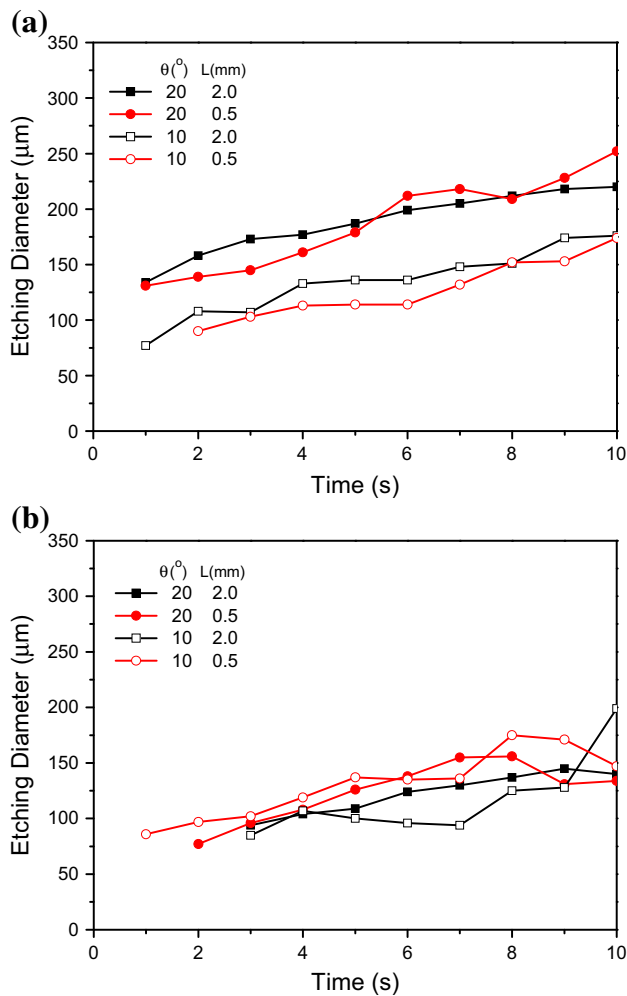


Fig. 7 Etching diameter for a conical nozzle with an outlet diameter of **a** 0.4 mm and **b** 0.6 mm

obtained was about 75–160 and 130–250 μm , respectively. Clearly, increasing the cone angle enhances the etching effect. As shown in Fig. 7b, for an outlet diameter of 0.6 mm, and a cone angle of 10° and 20°, the etching diameter obtained was about 75–180 μm .

3.3 Formation of cavity in the etching process

The formation of the etching cavity can be divided into three types: double-petal, triple-petal, and four-petal. Figures 8 and 9 show the SEM images of the cavity formation process at a laser power of 5 W at 2 kHz. Figure 8 presents the case of the cylindrical nozzle, where the nozzle depth is 0.5 mm and the outlet diameter is 0.25 mm. When a bubble collapses into two bubble jets and flows through the nozzle, the two bubble jets induce two etching pits on the glass surface. At the time of 2 s, the two etching pits of a diameter of < 30 μm were formed. Following the laser

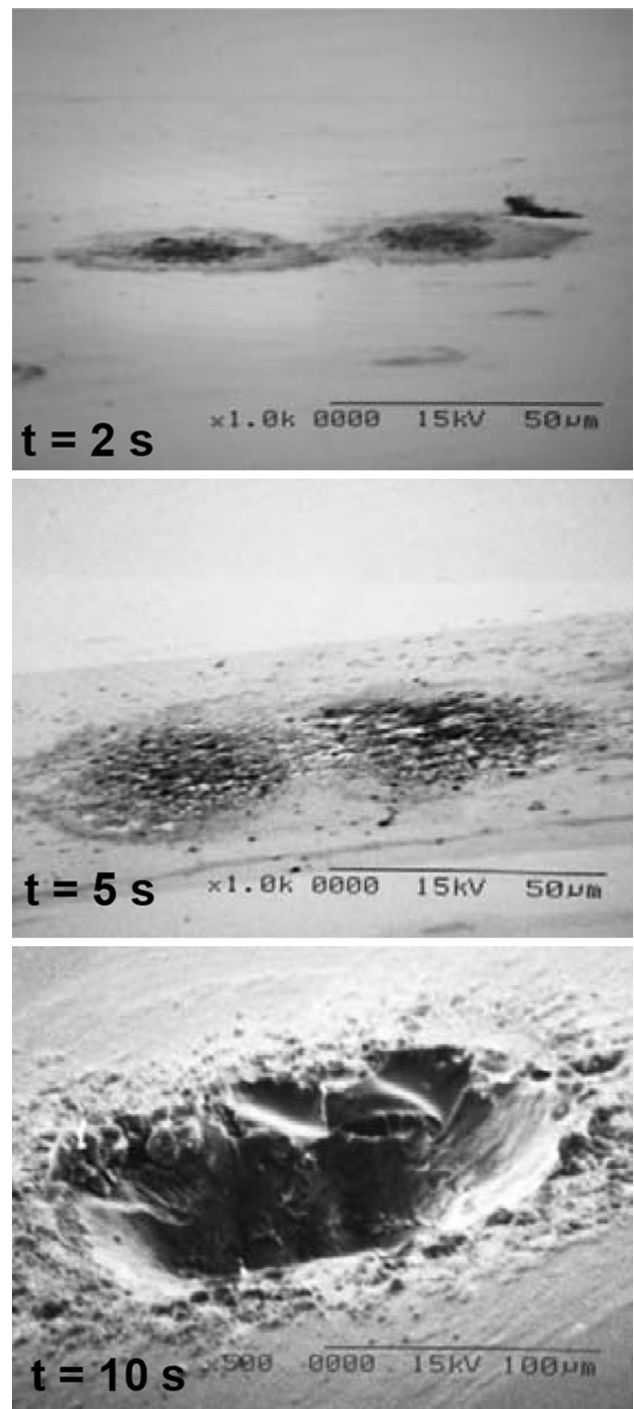
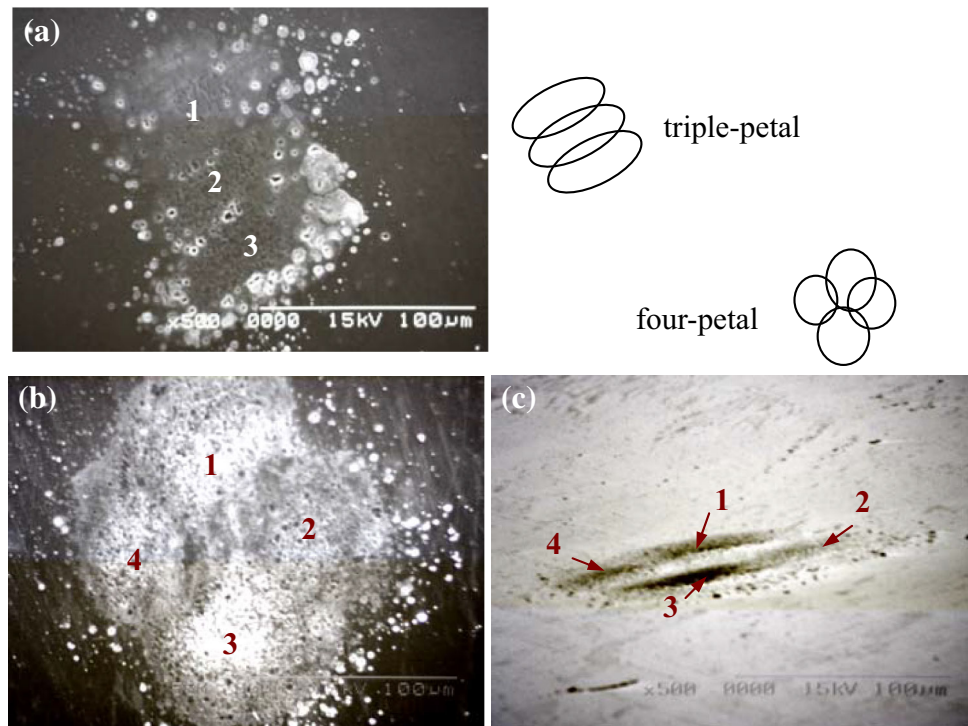


Fig. 8 Formation of the etching cavity during the laser etching process: double-petal type

application, the two etching pits expanded and combined to form a completed cavity.

Figure 9a gives the configuration and SEM images of triple-petal cavity formation for the cylindrical nozzle. The nozzle depth is 2 mm, and the outlet diameter is 0.25 mm. When a bubble collapses into three bubble jets and flows through the nozzle, the three bubble jets induce three

Fig. 9 Formation of the etching cavity during the laser etching process: **a** triple-petal type, four-petal type with the **b** top view and **c** oblique view



etching pits on the glass surface. The three etching pits then gradually expand and combine to form a completed cavity.

Figure 9b, c presents the configuration and SEM images of four-petal cavity formation for the conical nozzle. The nozzle depth is 0.5 mm, the outlet diameter is 0.4 mm, and the cone angle is 20°. When a bubble had collapsed into four bubble jets and flown through the nozzle, the four bubble jets induce four etching pits on the glass surface. The four etching pits gradually expand and combine to form a completed cavity.

One bubble jet induces one etching pit. The type of cavity formation depends on the jet number. When a bubble closes to a rigid hole, the bubble splits into two or more jets randomly; therefore, the type of cavity formation occurs randomly for each different experiment. In this study, both double-petal and triple-petal cavities were obtained with both cylindrical and conical nozzles. Only the conical nozzle produced a four-petal cavity.

4 Conclusion

Laser-induced backside wet etching technique using an Nd:YAG laser was successfully demonstrated for etching a cavity of 5–20 μm in depth and 50–250 μm in diameter on a glass surface. The needed laser power does not exceed 5 W. The impact of the bubble jet roughens the glass

surface and increases the absorption of laser energy. The softened glass material is expelled by the shock wave resulting from the jet impact. The bubble nozzles were found to enhance the strength of the bubble jet impact and confine the jetting direction. The proposed technique can prevent thermal damage and has great potential as an improved solution for the micro-machining of glass.

Acknowledgments The authors gratefully acknowledge the financial support of this research by the National Science Council (Taiwan) under Grant NSC 102-2221-E-211-001 to Huaan University.

References

1. L. Chen, J. Chuang, G.S. Mathad, U.S. Patent 4,478,677 (1984)
2. J. Ihlemann, B. Wolff, P. Simon, *Appl. Phys. A* **54**, 363 (1992)
3. J. Wang, H. Niino, A. Yabe, *Appl. Phys. A* **68**, 111 (1999)
4. J. Wang, H. Niino, A. Yabe, *Appl. Phys. A* **69**, S271 (1999)
5. K. Zimmer, A. Braun, R. Böhme, *Appl. Surf. Sci.* **208–209**, 199 (2003)
6. Z.Q. Huang, M.H. Hong, K.S. Tiaw, Q.Y. Lin, *J. Laser Micro Nanoeng.* **2**, 194 (2007)
7. G. Kopitkovas, T. Lippert, J. Venturini, C. David, A. Wokaun, *J. Phys: Conf. Ser.* **59**, 526 (2007)
8. K. Zimmer, R. Böhme, *Laser Chem.* **2008**, 1 (2008)
9. K. Zimmer, M. Ehrhardt, R. Böhme, *J. Appl. Phys.* **107**(1–8), 034908 (2010)
10. B. Hopp, C. Vass, T. Smausz, Z. Bor, *J. Phys. D Appl. Phys.* **39**, 4843 (2006)
11. B. Hopp, T. Smausz, C. Vass, G. Szabó, R. Böhme, D. Hirsch, K. Zimmer, *Appl. Phys. A* **94**, 899 (2009)

12. T. Smausz, T. Csizmadia, N. Kresz, C. Vass, Z. Márton, B. Hopp, *Appl. Surf. Sci.* **254**, 1091 (2007)
13. D.P. Banks, K.S. Kaur, R.W. Eason, *Appl. Surf. Sci.* **255**, 8343 (2009)
14. K. Zimmer, R. Böhme, C. Vass, B. Hopp, *Appl. Surf. Sci.* **255**, 9617 (2009)
15. Z. Tóth, M. Bereznai, K. Piglmayer, *Appl. Surf. Sci.* **208**, 205–209 (2003)
16. C. Hnatovsky, R.S. Taylor, E. Simova, P.P. Rajeev, D.M. Rayner, V.R. Bhardwaj, P.B. Corkum, *Appl. Phys. A* **84**, 47 (2006)
17. O. Yavas, A. Schilling, J. Bischof, J. Boneberg, P. Leiderer, *Appl. Phys. A* **64**, 331 (1997)
18. Y. Dou, L.V. Zhigilei, N. Winograd, B.J. Garrison, *J. Phys. Chem. A* **105**, 2748 (2001)
19. V. Lazic, J.J. Laserna, S. Jovicevic, *Spectrochim. Acta B At. Spectrosc.* **82**, 42 (2013)
20. V. Lazic, J.J. Laserna, S. Jovicevic, *Spectrochim. Acta B At. Spectrosc.* **82**, 50 (2013)
21. A. Takamizawa, S. Kajimoto, J. Hobley, K. Hatanaka, K. Ohta, H. Fukumura, *Phys. Chem. Chem. Phys.* **5**, 888 (2003)
22. A. Nath, A. Khare, *Laser Part. Beams* **29**, 1 (2011)
23. E.A. Brujan, K. Nahen, P. Schmidt, A. Vogel, *J. Fluid Mech.* **433**, 251 (2001)
24. E.A. Brujan, G.S. Keen, A. Vogel, J.R. Blake, *Phys. Fluids* **14**, 85 (2002)
25. B. Wolfrum, T. Kurz, R. Mettin, W. Lauterborn, *Phys. Fluids* **15**, 2916 (2003)
26. L.W. Chew, E. Klaseboer, S.W. Ohl, B.C. Khoo, *Exp. Therm. Fluid Sci.* **44**, 108 (2013)
27. B.C. Khoo, E. Klaseboer, K.C. Hung, *Sens. Actuators, A* **118**, 152 (2005)
28. K.S.F. Lew, E. Klaseboer, B.C. Khoo, *Sens. Actuators, A* **133**, 161 (2007)
29. V. Lazic, S. Jovicevic, M. Carpanese, *Appl. Phys. Lett.* **101**, 054101 (2012)